Pramana – J. Phys. (2019) 92:22
https://doi.org/10.1007/s12043-018-1677-z

Instability analysis of a streaming electrified cylindrical sheet through porous media

G M MOATIMID[1], Y O EL-DIB[1] and M H ZEKRY[2],*

[1]Department of Mathematics, Faculty of Education, Ain Shams University, Roxy, Cairo, Egypt
[2]Department of Mathematics and Computer Science, Faculty of Science, Beni-Suef University, Beni-Suef, Egypt
*Corresponding author. E-mail: marwa.zekry@science.bsu.edu.eg

MS received 1 March 2018; revised 29 April 2018; accepted 12 June 2018; published online 2 January 2019

Abstract. The current study deals with the influence of a uniform electric field on a cylindrical streaming sheet. This paper investigates a few representatives of porous media. These media are considered to be uniform, homogeneous and isotropic. The analysis is based on viscous potential theory, which assumes that the viscous forces affect only the interface between the fluids. The mathematical treatment is based on the normal modes analysis. For convenience, cylindrical coordinates are used. The boundary-value problem yields coupled second-order and damped differential equations with complex coefficients. These equations are combined with a single equation under the concepts of the symmetric and antisymmetric deformations. The Routh–Hurwitz criterion is adopted to govern the stability of the system. Several special cases are recovered upon appropriate data choices. The effects of various parameters on the interfacial stability are theoretically presented and illustrated graphically through some sets of figures. These parameters are the Darcy's coefficients, basic velocities, dielectric constants, viscosity and thickness of the inner cylinder. We have found that the thickness of the inner cylinder plays a dual role on the stability picture. Also, the Darcy's coefficient and dielectric constants have stabilising influence and the dynamic viscosity has a destabilising effect.

Keywords. Linear jets instability; electric field; porous media; viscous potential flow.

PACS Nos **68.05.Cf; 47.20.−k; 47.56.+r**

1. Introduction

The instability of liquid jets is important due to their wide range of applications, which involve liquid fuel injection, coating, drug delivery, food preparation and ink-jet printing. Eggers and Villermaux [1] introduced a good review to provide a unified description of the fundamental and technological aspects of these topics. Amini *et al* [2] studied the temporal linear stability of elliptic liquid jets. Their analysis was both theoretical and experimental. In comparison with the circular jet, they showed that the elliptic jet increases the growth rate over a large range of wave numbers. Chandrasekhar [3] proved that the jet is unstable for all axisymmetric perturbations having wave numbers less than unity. Meanwhile, for non-axisymmetric perturbations, it is permanently stable. In addition, Chandrasekhar [3] found that if the fluid is bounded by two cylindrical interfaces with radii a and b ($a < b$), the fluid is stable if both ka and kb (k is the wave number) are greater than unity. Seadawy and El-Rashidy [4] have investigated the nonlinear Rayleigh–Taylor instability of a cylindrical flow with mass and heat transfer. Their analysis resulted in Ginzburg–Landau equation. Also, they obtained an exact solution for this equation using the F-expansion method.

The electrohydrodynamic (EHD) stability flows have wide applications ranging from electrokinetic assays to electrospray ionisation. Chen [5] has introduced a few basic concepts of EHD instability. In the notes of his lectures, Chen used two model problems: electrokinetic mixing flow and EHD cone jet. Theoretical predictions of the non-axisymmetric instability growth rate of an EHD jet are studied by Korkut *et al* [6]. Elsayed *et al* [7] investigated the axisymmetric and asymmetric instabilities of a non-Newtonian liquid jet through porous media. They showed that the instability behaviour of the jet is influenced by the interaction of liquid viscosity, porous

medium parameters and elasticity. Also, they plotted sets of diagrams for the stability/instability of various physical parameters of the systems. Moatimid [8] investigated the instability of a nonlinear surface wave in an electrified liquid jet. His boundary-value problem leads to a non-linear characteristic second-order differential equation. Stability criteria are theoretically expressed in terms of various parameters of the system.

Flow through porous media has been of considerable interest in recent decades in many branches, particularly, among geophysical fluid dynamics, chemical engineering and petroleum industry. A good review in this area is given by Vafai [9]. The instability of a cylindrical interface between two uniform streaming porous media has been recently investigated by El-Sayed *et al* [7,10]. They found that various parameters of the porous media play a main role in the stability picture. The nonlinear instability of finitely conducting cylindrical flows through porous media is studied by Elcoot and Moatimid [11]. They showed that if the influence of Darcy's coefficient ratio between the two fluids satisfy certain conditions, the Darcian formulation allows an instability. Moatimid [12] investigated the instability of a cylindrical interface between two uniform fluids through porous media. He found that the porous parameters have destabilising influence. In addition, this influence is enhanced when the Darcy's coefficients are different. El-Sayed *et al* [7] investigated the axisymmetric and asymmetric instability of a non-Newtonian liquid jet through porous media. They found that the porosity of porous medium and the medium permeability have stabilising influences. Moreover, they showed that the system is more unstable in the presence of porous medium than in its absence.

Viscous potential flow (VPF) represents a good approximation to viscous theory in which it neglects the vorticity and friction over all the bluck of the fluid. In accordance, the viscous effects occur only at the interface between the two fluids. In other words, for the potential flow $\underline{v} = -\nabla\varphi$ gives a solution of the Navier–Stokes equations in viscous incompressible fluids at which the vorticity is identically zero. Also, the viscous term $\mu\nabla^2\varphi$ vanishes. Joseph [13] has introduced historical notes for the potential flow theory. In this review, he attempted to introduce main events in the irrotational flow of viscous fluids. Also, he demonstrated that every theorem of potential flow, with conservative body forces, applies equally to viscous fluids for regions of an irrotational flow. The instability of an EHD viscous liquid jets through porous media is investigated by Moatimid and Hassan [14]. They found that the increase in both the temperature and concentration at the axial microcylinder has a destabilising effect on the interface. Also, the existence of the porous structure restricts the flow and has a stabilising influence. Moatimid *et al* [15] studied the nonlinear EHD Kelvin–Helmholtz instability of an interface between two porous layers. They obtained a general dispersion relation in the view of the linear stability approach. Meanwhile, they deduced a Ginzburg–Landau equation in accordance with the nonlinear theory. Moatimid and Hassan [16] discussed the VPF in their work. Awasthi [17] has done a nonlinear analysis of the instability of a cylindrical interface with mass and heat transfer. They considered the theory of VPF in porous media. They observed that the heat and mass transfer and porous media both stabilise the interface. In contrast, the porosity supports a growth in wave disturbance. Li *et al* [18] studied the stability of an interface between two superposed viscous fluids in a channel subjected to a normal electric field. The effect of various parameters on the stability of their model is presented and illustrated using some sets of figures.

In this work, the stability of two cylindrical interfaces separating three dielectric fluids, which are affected by a tangential uniform electric field, is studied. The problem at hand considers the VPF together with the influence of porous media. This problem meets its great practical interest from a geophysical standpoint. Therefore, we have considered a simplified mathematical formulation of the problem of interfacial two cylindrical interfaces. This study examines a few representative porous media configurations. The influence of tangential periodic electric fields shall appear in a subsequent paper. To clarify the model, the paper is organised as follows: in §2, we describe the formulation of the problem including basic equations of motion and the perturbation analysis from the point of view of a linear stability theory. Section 3 is devoted to the introduction of linear boundary conditions of the problem. The linear stability analysis is given in §4. Three special cases are considered in §5. The first case is related to the stability analysis in the case of non-streaming, pure inviscid fluid in the absence of porous media; the second one considers a non-streaming, viscous fluid in the absence of porous media and the third case considers a non-streaming, viscous fluid in the porous media. Section 6 is devoted to studying the stability analysis on the general case. In this section, the transition curves are derived and the stability diagrams are plotted in accordance with numerical estimations. Finally, in §7, we give concluding remarks which are based on the obtained results of the stability analysis.

2. Mathematical formulation

Consider a system consisting of infinitely long liquid circular cylinders. The inner cylinder represents a rigid

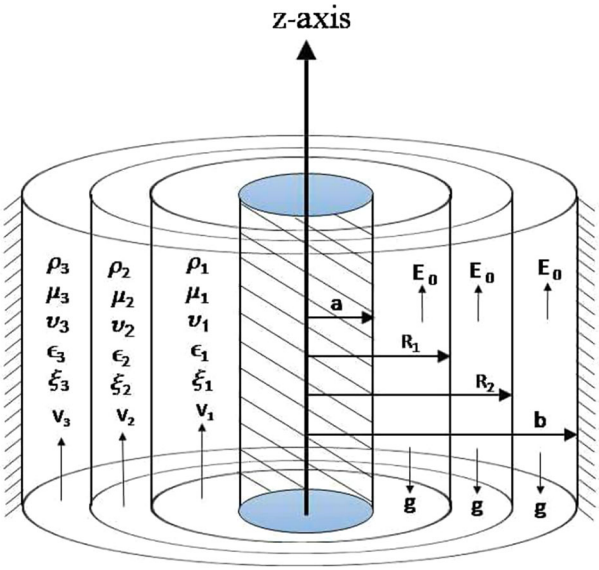

Figure 1. Sketch of an undisturbed system.

cylinder whose cross-section is of radius a, and the outer one is also rigid and of radius b. Three viscous dielectric fluids are separated by the hypothesised cylindrical interfaces $r = R_1$ and $r = R_2$. It is assumed that there are no volume charges in the three layers. Also, surface charges are absent at the interfaces. The fluids have been acted upon by an axial uniform electric field E_0. The inner, medium and outer liquids are incompressible and have uniform densities ρ_1, ρ_2 and ρ_3, respectively, from the inner to the outer direction. All the three liquids are fully saturated, uniform, homogeneous and isotropic porous media with Darcy's coefficients ν_1, ν_2 and ν_3 and porosity coefficients ξ_1, ξ_2 and ξ_3, respectively. The dynamic viscosity coefficients are μ_1, μ_2 and μ_3. The dielectric constants are ϵ_1, ϵ_2 and ϵ_3. Generally, the subsuffix (i) stands for the inner fluid, (ii) for the middle and (iii) for the outer one. The liquids are basically streaming with uniform velocities V_1, V_2 and V_3. The cylindrical polar coordinates (r, θ, z) are considered, so that in the equilibrium state, the z-axis could represent the axis of symmetry of the system. A schematic diagram of the configuration in the steady state is given in figure 1.

In the light of a normal modes analysis [3], the surface deflections $\eta_j(\theta, z; t)$ is given by a sinusoidal wave of finite amplitude as

$$\eta_j(\theta, z; t) = \gamma_j(t)\, \mathrm{e}^{\mathrm{i}(kz+m\theta)} + \text{c.c.}, \quad j = 1, 2, \tag{2.1}$$

where $\gamma_1(t)$ and $\gamma_2(t)$ are the arbitrary functions of time which determine the behaviour of the amplitude of disturbance on the interfaces. In addition, k is an axial wave number which is assumed to be real and positive, m is the azimuthal wave number, which is assumed to be positive and integer, and c.c. represents the complex conjugate of the proceeding term.

As shown from several foregoing works, e.g. of Chandrasekhar [3], the liquid jet is stable for all asymmetric modes, but it is unstable for axisymmetric modes. As a result, the most interesting mode of disturbance is the axisymmetric mode. In spite of this fact, the present study will consider a general case in the asymmetric modes.

The equations that give the motion of the problem at hand may be listed as follows.

The balance of the linear momentum of the viscous fluids through porous media according to Brinkman–Darcy equation is given by

$$\frac{\rho_j}{\xi_j}\left(\frac{\partial v_j}{\partial t} + \frac{1}{\xi_j}(v_j.\nabla)v_j\right) = -\nabla P_j + \mu_j \nabla^2 v_j - \nu_j v_j - \rho_j g \underline{e}_z, \quad j = 1, 2, 3, \tag{2.2}$$

where $v_j = v_j(r, z; t)$ is the fluid velocity and P_j is the pressure.

The static solution of eq. (2.2) yields

$$P_{0j} = -(\rho_j g + \nu_j V_j)z + \lambda_j, \tag{2.3}$$

where λ_j is an arbitrary time-dependent function.

In accordance with the incompressibility condition, we have

$$\frac{\partial v_j}{\partial x_j} = 0. \tag{2.4}$$

In EHD problems, the quasistatic approximation is usually considered [19]. In this case, the Maxwell's equations become

$$\nabla \wedge \underline{E}_j = 0 \tag{2.5}$$

and

$$\nabla.\epsilon_j \underline{E}_j = 0. \tag{2.6}$$

As the electric field is conservative, we may assume an electric potential $\psi_j = \psi_j(r, \theta, z; t)$ such that

$$\underline{E}_j = E_0 \underline{e}_z - \nabla \psi_j, \tag{2.7}$$

where $\underline{e}_z$ is a unit vector along the axis of the co-axial cylinders.

The combination of eqs (2.6) and (2.7) yields

$$\nabla^2 \psi_j = 0. \tag{2.8}$$

In analogy with the normal modes technique, we may assume that

$$\psi_j(r, \theta, z; t) = \hat{\psi}_j(r, t)\, \mathrm{e}^{\mathrm{i}(kz+m\theta)} + \text{c.c.} \tag{2.9}$$

In accordance with eq. (2.8), the unknown function $\hat{\psi}_j(r, t)$ satisfies the Bessel differential equation. Therefore, one gets

$$\hat{\psi}_j(r, t) = (C_j(t) I_m(kr) + D_j(t) K_m(kr)), \tag{2.10}$$

where $C_j(t)$ and $D_j(t)$ are the arbitrary time-dependent functions to be evaluated by using appropriate boundary conditions. In addition, $I_m(kr)$ and $K_m(kr)$ are the modified Bessel functions of the first and second kinds, respectively.

The function $S_j(r, \theta, z; t) = r - R_j - \eta_j$ $(j = 1, 2)$ as a geometrical surface function, where $S_j(r, \theta, z; t) = 0$ describes the wave-like profile of the disturbed interface. Therefore, the disturbed interface is located at $r = R_j + \eta_j(\theta, z; t)$ and the unit outward normal to the interface is given by $n_j = \nabla S_j / |\nabla S_j|$

$$\underline{n}_j = \underline{e}_r - \mathrm{i}m\eta_j \underline{e}_\theta - \mathrm{i}k\eta_j \underline{e}_z, \tag{2.11}$$

where $\underline{e}_r$ and $\underline{e}_\theta$ are the unit vectors in the radial direction and azimuthal directions, respectively.

To examine the interfacial stability of the problem under consideration, three-dimensional disturbances are taken into account in the equations of motion as well as the boundary conditions. In accordance with the VPF theory, the flow is irrotational and obeys the Laplace equation. As a result of perturbation, the initial fluid velocity increases and permits to introduce a scalar potential function $\varphi_j(r, \theta, z; t)$ such that the total velocity field may be written as

$$\underline{v}_j = V_j \underline{e}_z - \nabla \varphi_j. \tag{2.12}$$

In view of eq. (2.1), we may write

$$\varphi_j(r, \theta, z; t) = \hat{\varphi}_j(r, t)\, \mathrm{e}^{\mathrm{i}(kz + m\theta)} + \text{c.c.} \tag{2.13}$$

Then incompressibility condition (2.13) yields the Bessel differential equation. Therefore, one gets

$$\hat{\varphi}_j(r, t) = (A_j(t) I_m(kr) + B_j(t) K_m(kr)), \tag{2.14}$$

where $A_j(t)$ and $B_j(t)$ are arbitrary time-dependent functions to be evaluated from the appropriate boundary conditions.

Direct integrations of the equations of motion yields the following pressure distribution:

$$P_j = \frac{\rho_j}{\xi_j}\left(\frac{\partial \varphi_j}{\partial t} + \frac{V_j}{\xi_j}\frac{\partial \varphi_j}{\partial z}\right) + \nu_j \varphi_j. \tag{2.15}$$

3. Boundary conditions

To complete the formulation of the problem at hand, the general solutions of the potentials ψ and φ as given in eqs (2.10) and (2.14) must be completely determined. This requires evaluating the arbitrary time-dependent functions that appear in these equations. For this purpose, the appropriate boundary conditions may be classified into two distinct categories as follows:

3.1 *At the rigid boundaries*

The normal velocities of the fluid must vanish, which require the following conditions:

$$\frac{\partial \varphi_1}{\partial r} = 0 \quad \text{at } r = a \tag{3.1}$$

and

$$\frac{\partial \varphi_3}{\partial r} = 0 \quad \text{at } r = b. \tag{3.2}$$

The tangential components of the electric potential must vanish in which

$$\frac{\partial \psi_1}{\partial z} = 0 \quad \text{at } r = a \tag{3.3}$$

and

$$\frac{\partial \psi_3}{\partial z} = 0 \quad \text{at } r = b. \tag{3.4}$$

3.2 *At the fluid–fluid interfaces*

The transition between the bulk materials occurs over a finite but thin region. In a continuum description, we approximate this as surface of discontinuity in material properties. In this case, the appropriate boundary conditions may be written as follows.

The conservation of mass across the interfaces yields

$$\frac{\mathrm{D}S_j}{\mathrm{D}t} = 0 \ \text{ at } \ r = R_j + \eta_j(\theta, z; t) \quad (j = 1, 2), \tag{3.5}$$

where $\mathrm{D}/\mathrm{D}t$ represents the material derivative operator.

The tangential components of the electric are continuous at the interface yield

$$\underline{n}_j \wedge \|\underline{E}_j\| = \underline{0}, \quad r = R_j + \eta_j(\theta, z; t) \quad (j = 1, 2), \tag{3.6}$$

where $\|\ \|$ represents the difference (jump) in a quantity as we cross the interface, i.e. $\|f\| = f_2 - f_1$, where the subscripts refer to two different media.

It should be noted that condition (3.6) will be applied twice at $r = R_j + \eta_j(\theta, z; t)$ $(j = 1, 2)$.

Under the assumption that there is no surface currents at the interfaces, it follows that the normal components of the electric displacement ($\underline{D} = \epsilon \underline{E}$) are continuous at the interfaces. This yields

$$\underline{n}_j \cdot (\epsilon_j \underline{E}_j - \epsilon_{j+1} \underline{E}_{j+1}) = 0 \quad \text{at } \ r = R_j + \eta_j(\theta, z; t). \tag{3.7}$$

At this stage, the considered boundary-value problem is completed. By direct substitution from eq. (2.3) into eqs (3.1), (3.2) and (3.5), the calculations are lengthy but straightforward, one gets

$$\varphi_1(r,\theta,z;t) = -\frac{2Q(r,a)}{k(M(R_1)L(a)-M(a)L(R_1))} \times (\mathrm{i}kV_1\gamma_1(t)+\gamma_1'(t))\,\mathrm{e}^{\mathrm{i}(kz+m\theta)} + \text{c.c.}, \tag{3.8}$$

$$\varphi_2(r,\theta,z;t) = \frac{2}{k(M(R_2)L(R_1)-M(R_1)L(R_2))} \times (Q(r,R_2)(\mathrm{i}kV_2\gamma_1(t)+\gamma_1'(t)) - Q(r,R_1)(\mathrm{i}kV_2\gamma_2(t) + \gamma_2'(t)))\,\mathrm{e}^{\mathrm{i}(kz+m\theta)} + \text{c.c.} \tag{3.9}$$

and

$$\varphi_3(r,\theta,z;t) = -\frac{2Q(r,b)}{k(M(R_2)L(b)-M(b)L(R_2))} \times (\mathrm{i}kV_3\gamma_2(t)+\gamma_2'(t))\,\mathrm{e}^{\mathrm{i}(kz+m\theta)} + \text{c.c.} \tag{3.10}$$

The constants $L(A_1)$, $M(A_1)$ and $Q(A_1, A_2)$ are given in Appendix A, A_1 and $A_2 = a, b, R_1, R_2$ and r.

Again, from eq. (2.12) into eqs (3.3), (3.4), (3.6) and (3.7), one finds

$$\psi_1(r,\theta,z;t) = \mathrm{i}E_0^2 P(a,r)(L_1\gamma_1(t) + L_2\gamma_2(t))\,\mathrm{e}^{\mathrm{i}(kz+m\theta)} + \text{c.c.}, \tag{3.11}$$

$$\psi_2(r,\theta,z;t) = \mathrm{i}E_0^2((P(r,R_1)L_3 + Q(r,R_1)L_4)\gamma_1(t) + (P(r,R_1)L_5 + Q(r,R_1)L_6)\gamma_2(t))\,\mathrm{e}^{\mathrm{i}(kz+m\theta)} + \text{c.c.} \tag{3.12}$$

and

$$\psi_3(r,\theta,z;t) = \mathrm{i}E_0^2 P(b,r)(L_7\gamma_1(t) + L_8\gamma_2(t))\,\mathrm{e}^{\mathrm{i}(kz+m\theta)} + \text{c.c.} \tag{3.13}$$

Again, the constants L_1–L_8 are given in Appendix A.

In accordance with the VPF, the viscous term enters only through the normal stress balance. As stated before, it is ignored throughout the linear momentum equation. Therefore, the various vorticities and circulation theorem of the inviscid potential flow are valid in VPF. The influences of electric field and viscosity are considered, only through the normal stress tensor balance at the interface and the viscosity is neglected elsewhere.

In order to complete the linear stability analysis, the remaining boundary condition arises from the normal component of the total stress tensor. This component is discontinuous at the interface by an amount of the surface tension.

The remaining condition may be formulated as follows.

The stress tensor of the viscous fluid [3] may be written as

$$\sigma_{ij}^{\mathrm{vis}} = -P\delta_{ij} + \mu\left(\frac{\partial v_i}{\partial x_j} + \frac{\partial v_j}{\partial x_i}\right), \tag{3.14}$$

where δ_{ij} is the Kronecker delta.

The stress tensor of the combined free charge and polarisation force densities [19] may be written as

$$\sigma_{ij}^{\mathrm{elec}} = \epsilon E_i E_j - \frac{1}{2}\epsilon E^2\delta_{ij}. \tag{3.15}$$

Therefore, the total stress tensor is given by

$$\sigma_{ij}^{\mathrm{tot}} = \sigma_{ij}^{\mathrm{vis}} + \sigma_{ij}^{\mathrm{elec}}. \tag{3.16}$$

The discontinuity of the normal stress tensor may be illustrated as

$$\underline{n}\cdot\|\underline{F}\| = T\left(\frac{1}{R_1}+\frac{1}{R_2}\right) \tag{3.17}$$

at the interface, where $\underline{F}$ is the total force acting on the interface, which is defined by

$$\underline{F} = \begin{bmatrix}\sigma_{rr} & \sigma_{r\theta} & \sigma_{rz}\\ \sigma_{\theta r} & \sigma_{\theta\theta} & \sigma_{\theta z}\\ \sigma_{zr} & \sigma_{z\theta} & \sigma_{zz}\end{bmatrix}\begin{bmatrix}n_r\\ n_\theta\\ n_z\end{bmatrix}, \tag{3.18}$$

where T is the amount of surface tension, R_1 and R_2 are the two principal radii of curvature, and n_r, n_θ and n_z are the components of the outward unit normal vector $\underline{n}$.

At the fluid interfaces, the following conditions must be held:

$$\underline{n}_j\cdot\|\underline{F}_j\| = T_{j(j+1)}\nabla^2 S_j,\quad r = R_j + \eta_j(\theta,z;t),\quad j=1,2. \tag{3.19}$$

By substituting the electric potential, velocity potential and pressure into the normal stress tension condition (3.19), one gets the zero-order of normal stress tensor

$$\lambda_1-\lambda_2 = (\rho_1-\rho_2)gz + (\nu_1V_1-\nu_2V_2)z - \frac{T_{12}}{R_1} \tag{3.20}$$

and

$$\lambda_2-\lambda_3 = (\rho_2-\rho_3)gz + (\nu_2V_2-\nu_3V_3)z - \frac{T_{23}}{R_2}. \tag{3.21}$$

The first order of normal stress tensor yields

$$P_2 - P_1 + E_0\left(\epsilon_1\frac{\partial\psi_1}{\partial z} - \epsilon_2\frac{\partial\psi_2}{\partial z}\right) - 2\left(\mu_1\frac{\partial^2\varphi_1}{\partial r^2} - \mu_2\frac{\partial^2\varphi_2}{\partial r^2}\right) - \frac{T_{12}}{R_1^2}(k^2R_1^2-1)\eta_1 = 0 \ \text{ at } \ r = R_1 + \eta_1(\theta,z;t) \tag{3.22}$$

and

$$P_3 - P_2 + E_0\left(\epsilon_2\frac{\partial\psi_2}{\partial z} - \epsilon_3\frac{\partial\psi_3}{\partial z}\right) - 2\left(\mu_2\frac{\partial^2\varphi_2}{\partial r^2} - \mu_3\frac{\partial^2\varphi_3}{\partial r^2}\right) - \frac{T_{23}}{R_2^2}(k^2R_2^2 - 1)\eta_2 = 0 \quad \text{at} \quad r = R_2 + \eta_2(\theta, z; t). \tag{3.23}$$

Again, the substitution of eqs (2.15), (3.8)–(3.13), (3.22) and (3.23), after lengthy but straightforward calculations, yields

$$k_{11}\ddot{\gamma}_1(t) + q_{22}\ddot{\gamma}_2(t) + (f_{11} + \mathrm{i}l_{11})\dot{\gamma}_1(t) + (s_{11} + \mathrm{i}h_{11})\gamma_1(t) + (f_{22} + \mathrm{i}l_{22})\dot{\gamma}_2(t) + (s_{22} + \mathrm{i}h_{22})\gamma_2(t) = 0 \tag{3.24}$$

and

$$q_{21}\ddot{\gamma}_1(t) + k_{12}\ddot{\gamma}_2(t) + (f_{12} + \mathrm{i}l_{12})\dot{\gamma}_2(t) + (s_{12} + \mathrm{i}h_{12})\gamma_2(t) + (f_{21} + \mathrm{i}l_{21})\dot{\gamma}_1(t) + (s_{21} + \mathrm{i}h_{21})\gamma_1(t) = 0. \tag{3.25}$$

$k_{1j}, f_{1j}, l_{1j}, s_{1j}, h_{1j}, q_{2j}, f_{2j}, l_{2j}, s_{2j}$ and h_{2j} are given in Appendix B.

Equations (3.24) and (3.25) are coupled linear second-order differential equations with damped and complex coefficients. These equations may be used to judge the linear stability of the infinite cylindrical sheet.

Similar equations for (3.24) and (3.25), were earlier obtained by El-Dabe *et al* [20].

4. Stability analysis

Let us first define the concept of symmetric and antisymmetric wave functions.

Construct wave function of a system of identical particles such that it reflects the requirement that the particle is indistinguishable from each other. Mathematically, this means that interchanging the particle occupying any pair of states should not change the probability density $|\chi|^2$ of the system.

Therefore, the probability density of the wave function $\chi(r_1, r_2)$ must be identical to that of the wave function $\chi(r_1, r_2)$, where the particle has been interchanged

$$|\chi(r_1, r_2)|^2 = |\chi(r_2, r_1)|^2. \tag{4.1}$$

This may be achieved in two ways as follows:

(i) Symmetric case $\chi(r_1, r_2) = \chi(r_2, r_1)$.
(ii) Antisymmetric case $\chi(r_1, r_2) = -\chi(r_2, r_1)$.

Now, to relax the complexity of the coupled equations (3.24) and (3.25), we use the concept of symmetric and antisymmetric metric deflections of the surface waves η_1 and η_2.

Therefore, let

$$\eta_2 = J\eta_1 = \eta, \tag{4.2}$$

where $J = 1$ represents the symmetric case and $J = -1$ represents the antisymmetric one.

Consider a simplified form as given in eq. (4.2) in the coupled eqs (3.24) and (3.25). Therefore, these characteristic equations are reduced to the following equations:

$$\ddot{\gamma}(t) + (F_1 + \mathrm{i}G_1)\dot{\gamma}(t) + (S_1 + \mathrm{i}H_1)\gamma(t) = 0, \tag{4.3}$$

$$\ddot{\gamma}(t) + (F_2 + \mathrm{i}G_2)\dot{\gamma}(t) + (S_2 + \mathrm{i}H_2)\gamma(t) = 0, \tag{4.4}$$

where

$$F_1 = \frac{f_{22} + Jf_{11}}{q_{22} + Jk_{11}}, \quad G_1 = \frac{l_{22} + Jl_{11}}{q_{22} + Jk_{11}},$$
$$S_1 = \frac{s_{22} + Js_{11}}{q_{22} + Jk_{11}}, \quad H_1 = \frac{h_{22} + Jh_{11}}{q_{22} + Jk_{11}},$$
$$F_2 = \frac{f_{12} + Jf_{21}}{k_{12} + Jq_{21}}, \quad G_2 = \frac{l_{12} + Jl_{21}}{k_{12} + Jq_{21}},$$
$$S_2 = \frac{s_{12} + Js_{21}}{k_{12} + Jq_{21}} \text{ and } H_2 = \frac{h_{12} + Jh_{21}}{k_{12} + Jq_{21}}.$$

The coupled differential equations (4.3) and (4.4) are combined by adding them to give one equation as follows:

$$\ddot{\gamma}(t) + (F_3 + \mathrm{i}G_3)\dot{\gamma}(t) + (S_3 + \mathrm{i}H_3)\gamma(t) = 0, \tag{4.5}$$

where $F_3 = \frac{1}{2}(F_1 + F_2)$, $G_3 = \frac{1}{2}(G_1 + G_2)$, $S_3 = \frac{1}{2}(S_1 + S_2)$ and $H_3 = \frac{1}{2}(H_1 + H_2)$.

Equation (4.5) is a linear homogeneous differential equation with complex coefficients. Therefore, the exponential solution is valid.

Hence, the solution of eq. (4.5) is written as

$$\gamma(t) = \delta\mathrm{e}^{-\mathrm{i}\omega t}, \tag{4.6}$$

where δ is a real constant and ω is of a complex nature in general.

From eqs (4.5) and (4.6), one gets

$$\omega^2 + \Lambda_1\omega + \Lambda_2 = 0, \tag{4.7}$$

where $\Lambda_1 = -G_3 + \mathrm{i}F_3$ and $\Lambda_2 = -S_3 - \mathrm{i}H_3$.

It should be noted that (4.7) represents a linear dispersion relation for the surface waves that propagate through the electrified streaming cylindrical sheet in the porous media. This dispersion relation is satisfied by the values of ω and k. Therefore, if the imaginary part of ω is positive, the disturbance will temporally grow with time and the flow will be unstable. On the other hand, if the imaginary part of ω is negative, the disturbances will decay with time and the flow becomes stable.

Before dealing with general case, it is convenient to consider the special case when the fluids are inviscid ($\mu_j = 0$) and also, for non-porous media where ($\nu_j = 0$ and $\xi_j = 1$) ($j = 1, 2, 3$). In this case, we obtain the previous characteristic equations that are given by El-Dabe *et al* [20] but in the case of uniform tangential electric field. It should be taken into account that the cases will be graphed, for simplicity, in the axisymmetric case.

5. Special cases

It is more convenient to discuss the stability analysis of some special cases in detail. These cases may be formulated as follows:

5.1 *For an inviscid, non-porous and non-streaming flow*

If we ignore each of the dynamic viscosities, streaming, Darcy's coefficients and considering the porosity of all media are unity, the dispersion relation (4.7) will be simplified in the form

$$\omega^2 - S_4 = 0, \tag{5.1}$$

where $S_4 = S_3$ at $\mu_j = 0$, $\nu_j = 0$, $\xi_j = 1$ and $V_j = 0$ ($j = 1, 2, 3$).

Therefore, the interfaces between the fluids are stable or unstable depending on whether ω is real or complex. As our aim is to study the amplitude modulation of the progressive waves, we assume that $\omega^2 > 0$.

Therefore, the system is linearly stable if

$$\alpha_1 E_0^2 + \beta_1 > 0. \tag{5.2}$$

α_1 and β_1 are given in Appendix C.

Before dealing with numerical estimations, it is convenient to write the above stability condition in an appropriate dimensionless form. This can be done in a number of ways depending primarily on the choice of the characteristic length, time and mass. Consider the following dimensionless forms: the characteristic length $= b$, the characteristic time $= \sqrt{b/g}$ and the characteristic mass $= \rho_2 b^3$. The other dimensionless quantities are given by

$$k = \frac{k^*}{b}, \quad a = a^* b, \quad R_1 = R_1^* b, \quad R_2 = R_2^* b,$$
$$\rho_1 = \rho_1^* \rho_2, \quad \rho_3 = \rho_3^* \rho_2, \quad E_0^2 = (E_0^2)^* \rho_2 g b,$$
$$T_{12} = T_{12}^* \rho_2 g b^2 \text{ and } T_{23} = T_{23}^* \rho_2 g b^2. \tag{5.3}$$

For simplicity, the '$*$' mark may be ignored in the following analysis.

The influence of electric field on stability depends mainly on the sign of the parameter α_1.

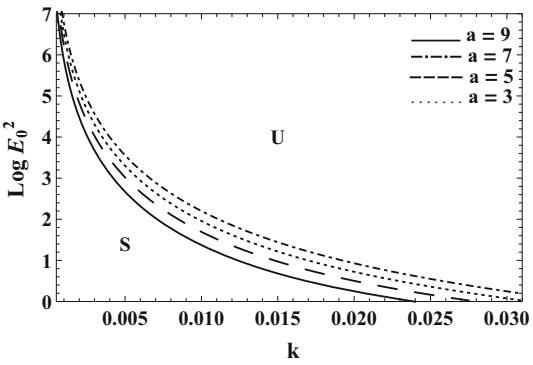

Figure 2. $\rho_1 = 0.3$, $\rho_3 = 1.9$, $\epsilon_1 = 2$, $\epsilon_2 = 0.9$, $\epsilon_3 = 5$, $R_1 = 10$, $R_2 = 20$, $T_{12} = 19$ and $T_{23} = 25$.

Generally, our interest is focussed on the relation between the electric field intensity $\log(E_0^2)$ and the wave number of the surface waves k. Therefore, the stability diagram is plotted for $\log(E_0^2)$ vs. the wave number k. In the following figures, the stable region is characterised by the letter S. Meanwhile, the letter U stands for the unstable region.

In what follows, a numerical calculation is performed for the given special case.

Figure 2 considers the symmetric case. In this figure, $\log(E_0^2)$ is plotted vs. the wave number k for various values of a, the radius of cross-section of the inner cylinder. The numerical calculation shows that the parameter α_1 is positive over all the given domains which illustrates again the stabilising influence of the tangential electric field. This figure depicts that the parameter a has a stabilising influence, especially at large values of the wave number k.

5.2 *For viscous, non-porous and non-streaming flow*

When neglecting the streaming, Darcy's coefficients and considering the porosity of all media to be unity, the dispersion relation (4.5) is written as follows:

$$\ddot{\gamma}(t) + F_4 \dot{\gamma}(t) + S_4 \gamma(t) = 0, \tag{5.4}$$

where $F_4 = F_3$ and $S_4 = S_3$ at $\nu_j = 0$, $\xi_j = 1$ and $V_j = 0$ ($j = 1, 2, 3$).

Let $\gamma(t) = \tau_1(t)\, \mathrm{e}^{-(1/2)F_4 t}$, eq. (5.4) is converted to

$$\ddot{\tau}_1(t) + \left(S_4 - \frac{F_4^2}{4}\right)\tau_1(t) = 0. \tag{5.5}$$

Let $\tau_1(t) = \tau_{01} \mathrm{e}^{-\mathrm{i}\omega t}$, where τ_{01} is an arbitrary real constant. This yields

$$\omega^2 - \left(S_4 - \frac{F_4^2}{4}\right) = 0. \tag{5.6}$$

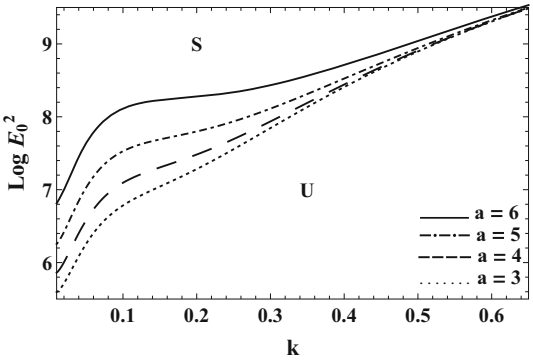

Figure 3. $\rho_1 = 0.3, \rho_2 = 0.5, \rho_3 = 1.9, \epsilon_1 = 2, \epsilon_2 = 0.9, \epsilon_3 = 5, R_1 = 10, R_2 = 20, T_{12} = 19, T_{23} = 25, \mu_1 = 1000$ and $\mu_3 = 500$.

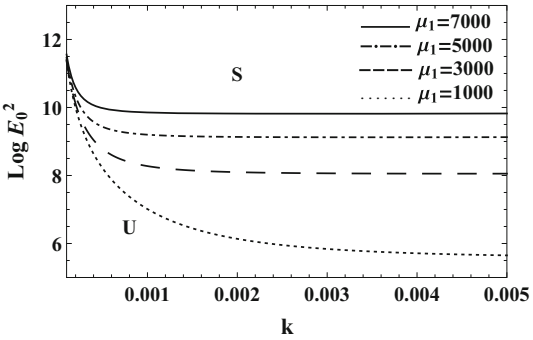

Figure 4. $a = 3, \rho_1 = 0.3, \rho_2 = 0.5, \rho_3 = 1.9, \epsilon_1 = 2, \epsilon_2 = 0.9, \epsilon_3 = 5, R_1 = 10, R_2 = 20, T_{12} = 19, T_{23} = 25$ and $\mu_3 = 500$.

The system is linearly stable if ω^2 is positive, $S_4 - (F_4^2/4)$ can be written in the form

$$4\alpha_1 E_0^2 + \beta_2 > 0, \tag{5.7}$$

where

$$\beta_2 = -F_4^2 + 4\beta_1,$$

under the restriction that F_4 must be positive.

Before dealing with numerical calculations, it is convenient to write the stability condition in an appropriate dimensionless form. Similar arguments will be used as in the previous case. It should be noted that the characteristics considered here are length $= b$, time $= \sqrt{b/g}$ and mass $= \mu_2 b\sqrt{b/g}$.

In what follows, a numerical calculation, for the symmetric case, is performed for the given special case.

As before, the present calculation shows that parameter α_1 is always positive. In contrast with figure 2, the parameter a has a destabilising influence in figure 3. Figure 4 is depicted to indicate the influence of dynamic viscosity μ_1 on the stability behaviour. The figure shows the destabilising influence of this parameter, especially, at large values of the wave number k.

5.3 *For viscous, non-streaming flow in porous media*

In the absence of streaming fluids, the dispersion relation (4.5) is written as follows:

$$\ddot{\gamma}(t) + F_3\dot{\gamma}(t) + S_4\gamma(t) = 0. \tag{5.8}$$

Equation (5.8) in a normal form is transformed to the following form:

$$\ddot{\tau_2}(t) + \left(S_4 - \frac{F_3^2}{4}\right)\tau_2(t) = 0, \tag{5.9}$$

under the transformation

$$\gamma(t) = \tau_2(t)\,\mathrm{e}^{-(1/2)F_3 t}. \tag{5.10}$$

Let $\tau_2(t) = \tau_{02}\mathrm{e}^{-\mathrm{i}\omega t}$, where τ_{02} is the arbitrary real constant. Equation (5.9) then becomes

$$\omega^2 - \left(S_4 - \frac{F_3^2}{4}\right) = 0. \tag{5.11}$$

The system is linearly stable if ω^2 is positive, and

$$4\alpha_1 E_0^2 + \beta_3 > 0, \tag{5.12}$$

where $\beta_3 = -F_3^2 + 4\beta_1$. We shall consider the same dimensionless quantities as given in the case presented in §5.2.

It should be noted that F_3 is independent of the electric field intensity. In fact, the restriction on F_3 must be taken into account when considering the stability picture.

In what follows, a numerical calculation, for the symmetric case, is performed for the given special case.

As before, the present calculations show that parameter α_2 is always positive. In contrast with figures 2 and 3, in figure 5, the parameter a has a dual role in the stability picture. Figure 6 is depicted to indicate the influence of Darcy's coefficient ν_2 on the stability behaviour. The Darcy's coefficient has a dual role in the stability figure.

6. The general case

Equation (4.7) is an algebraic quadratic equation with complex coefficients. As stated above, the stability criteria depend mainly on the nature of the frequency ω. According to the Routh–Hurwitz criteria [21], the necessary and sufficient stability conditions for (4.7) are

$$\mathrm{Re}(\Lambda_1) > 0 \tag{6.1}$$

and

$$\mathrm{Re}(\Lambda_1)\mathrm{Re}(\Lambda_1\bar{\Lambda}_2) - (\mathrm{Im}\Lambda_2)^2 > 0. \tag{6.2}$$

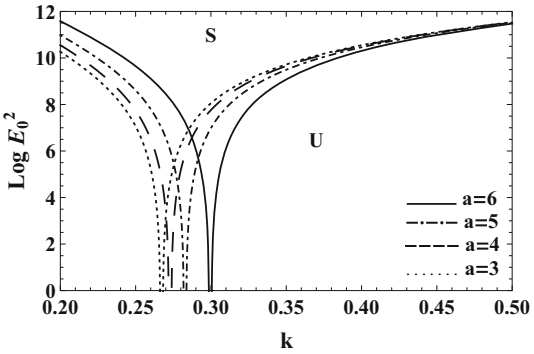

Figure 5. $\rho_1 = 0.3, \rho_2 = 0.5, \rho_3 = 1.9, \xi_1 = 0.3, \xi_2 = 0.02, \xi_3 = 0.6, \epsilon_1 = 2, \epsilon_2 = 0.9, \epsilon_3 = 5, R_1 = 10, R_2 = 20, T_{12} = 19, T_{23} = 25, \mu_1 = 1000, \mu_3 = 500, \nu_1 = 1000, \nu_2 = 500$ and $\nu_3 = 600$.

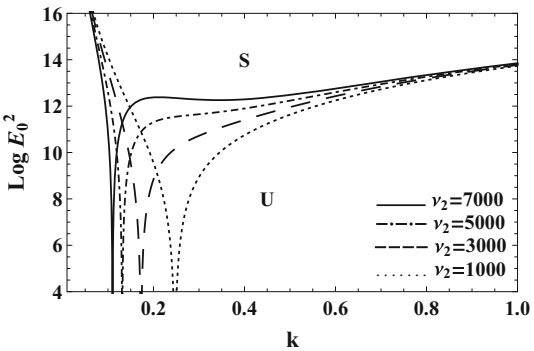

Figure 6. $a = 3, \rho_1 = 0.3, \rho_2 = 0.5, \rho_3 = 1.9, \xi_1 = 0.3, \xi_2 = 0.02, \xi_3 = 0.6, \epsilon_1 = 2, \epsilon_2 = 0.9, \epsilon_3 = 5, R_1 = 10, R_2 = 20, T_{12} = 19, T_{23} = 25, \mu_1 = 1000, \mu_3 = 500, \nu_1 = 1000$ and $\nu_3 = 600$.

With regard to the coefficients of the characteristic eq. (4.7), Routh–Hurwitz criteria may be written as

$$G_3 < 0 \tag{6.3}$$

and

$$\alpha E_0^2 + \beta < 0, \tag{6.4}$$

where $\alpha = \alpha_1 G_3^2$ and β is given in Appendix C.

In what follows, we shall consider the same dimensionless quantities as given in the case presented in §5.2.

The first condition (6.3) is independent of the electric field intensity. In fact, this condition must be taken into account while considering the stability picture.

In what follows, a numerical calculation, for symmetric case ($J = 1$), is performed and for the axisymmetric mode ($m = 0$) in the general case.

As stated before, the implication of condition (6.3) must be considered. All the following figures are plotted for a domain of the wave number such that condition (6.3) is automatically satisfied. In addition, all the present calculations indicated that the parameter α is always of negative sign. This shows, again, that the electric field intensity has a stabilising influence, which is a fact proved by many research studies.

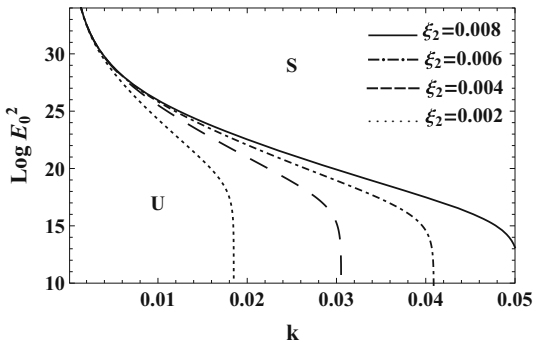

Figure 7. $a = 3, \rho_1 = 0.3, \rho_2 = 0.5, \rho_3 = 1.9, \xi_1 = 0.03, \xi_3 = 0.6, V_1 = 0.3, V_2 = 0.5, V_3 = 30, \epsilon_1 = 2, \epsilon_2 = 0.9, \epsilon_3 = 5, R_1 = 10, R_2 = 20, T_{12} = 19, T_{23} = 25, \mu_1 = 1000, \mu_3 = 500, \nu_1 = 1000, \nu_2 = 100$ and $\nu_3 = 600$.

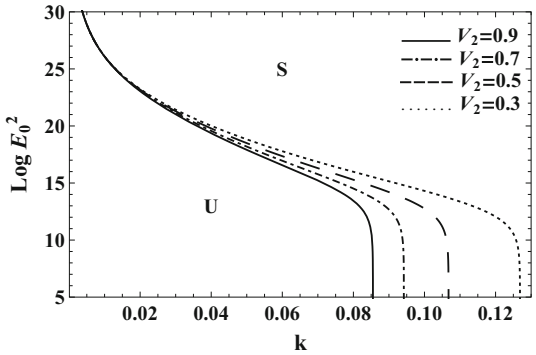

Figure 8. $a = 3, \rho_1 = 0.3, \rho_2 = 0.5, \rho_3 = 1.9, \xi_1 = 0.03, \xi_2 = 0.02, \xi_3 = 0.6, V_1 = 0.3, V_3 = 30, \epsilon_1 = 2, \epsilon_2 = 0.9, \epsilon_3 = 5, R_1 = 10, R_2 = 20, T_{12} = 19, T_{23} = 25, \mu_1 = 1000, \mu_3 = 500, \nu_1 = 1000, \nu_2 = 100$ and $\nu_3 = 600$.

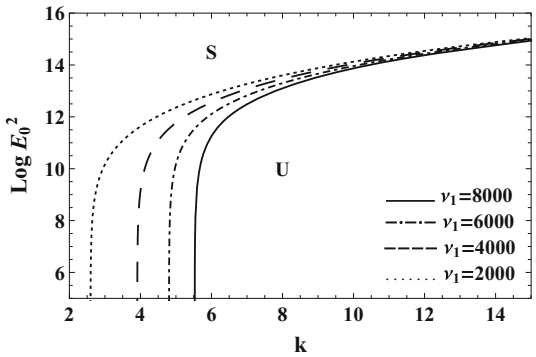

Figure 9. $a = 3, \rho_1 = 0.3, \rho_2 = 0.5, \rho_3 = 1.9, \xi_1 = 0.03, \xi_2 = 0.02, \xi_3 = 0.6, V_1 = 0.3, V_2 = 0.5, V_3 = 30, \epsilon_1 = 2, \epsilon_2 = 0.9, \epsilon_3 = 5, R_1 = 10, R_2 = 20, T_{12} = 19, T_{23} = 25, \mu_1 = 1000, \mu_3 = 500, \nu_2 = 100$ and $\nu_3 = 600$.

From figure 7, the influence of porosity of the middle fluid ξ_2 is depicted. Therefore, $\log(E_0^2)$ is plotted

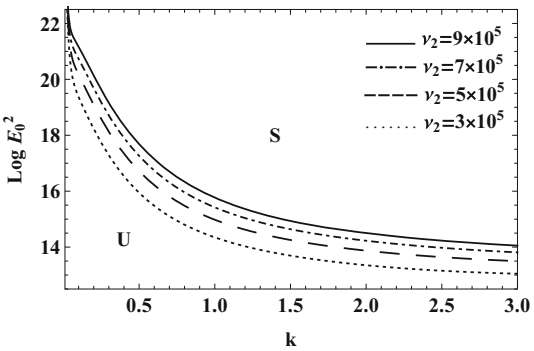

Figure 10. $a = 3$, $\rho_1 = 0.3$, $\rho_2 = 0.5$, $\rho_3 = 1.9$, $\xi_1 = 0.03$, $\xi_2 = 0.02$, $\xi_3 = 0.6$, $V_1 = 0.3$, $V_2 = 0.5$, $V_3 = 30$, $\epsilon_1 = 2$, $\epsilon_2 = 0.9$, $\epsilon_3 = 5$, $R_1 = 10$, $R_2 = 20$, $T_{12} = 19$, $T_{23} = 25$, $\mu_1 = 1000$, $\mu_3 = 500$, $\nu_1 = 1000$ and $\nu_3 = 600$.

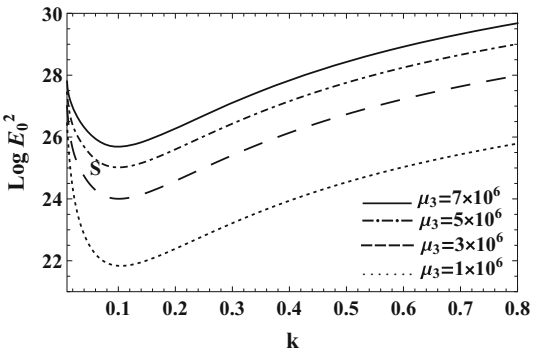

Figure 11. $a = 3$, $\rho_1 = 0.3$, $\rho_2 = 0.5$, $\rho_3 = 1.9$, $\xi_1 = 0.03$, $\xi_2 = 0.02$, $\xi_3 = 0.6$, $V_1 = 0.3$, $V_2 = 0.5$, $V_3 = 30$, $\epsilon_1 = 2$, $\epsilon_2 = 0.9$, $\epsilon_3 = 5$, $R_1 = 10$, $R_2 = 20$, $T_{12} = 19$, $T_{23} = 25$, $\mu_1 = 1000$, $\nu_1 = 1000$, $\nu_2 = 100$ and $\nu_3 = 600$.

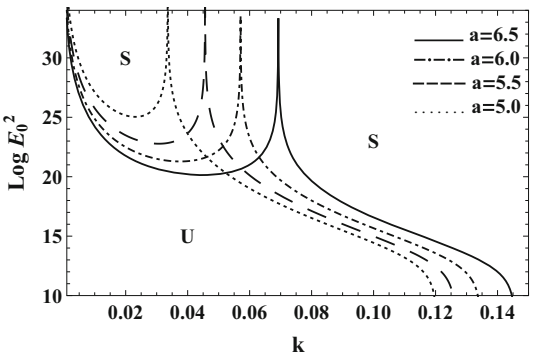

Figure 12. $\rho_1 = 0.3$, $\rho_2 = 0.5$, $\rho_3 = 1.9$, $\xi_1 = 0.03$, $\xi_2 = 0.02$, $\xi_3 = 0.6$, $V_1 = 0.3$, $V_2 = 0.5$, $V_3 = 30$, $\epsilon_1 = 2$, $\epsilon_2 = 0.9$, $\epsilon_3 = 5$, $R_1 = 10$, $R_2 = 20$, $T_{12} = 19$, $T_{23} = 25$, $\mu_1 = 1000$, $\mu_3 = 500$, $\nu_1 = 1000$, $\nu_2 = 100$ and $\nu_3 = 600$.

vs. the wave number k according to different values of ξ_2 and porosity has a destabilising effect, especially, at large values of k. Figure 8 depicts the influence of the variation of streaming V_2 in the stability figure. The figure in which $V_1 \leq V_2 < V_3$ is plotted. It is shown that

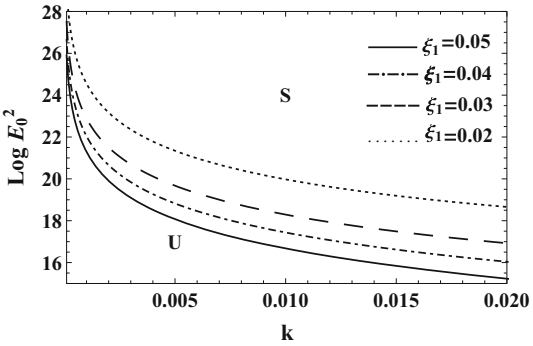

Figure 13. $a = 3$, $\rho_1 = 0.3$, $\rho_2 = 0.5$, $\rho_3 = 1.9$, $\xi_2 = 0.2$, $\xi_3 = 0.6$, $V_1 = 0.3$, $V_2 = 0.5$, $V_3 = 30$, $\epsilon_1 = 2$, $\epsilon_2 = 0.9$, $\epsilon_3 = 5$, $R_1 = 10$, $R_2 = 20$, $T_{12} = 19$, $T_{23} = 25$, $\mu_1 = 1000$, $\mu_3 = 500$, $\nu_1 = 1000$, $\nu_2 = 100$ and $\nu_3 = 600$.

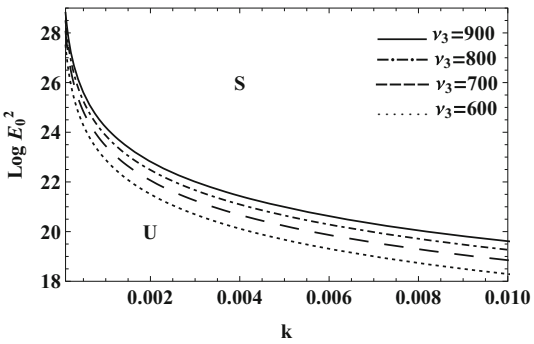

Figure 14. $a = 3$, $\rho_1 = 0.3$, $\rho_2 = 0.5$, $\rho_3 = 1.9$, $\xi_1 = 0.03$, $\xi_2 = 0.02$, $\xi_3 = 0.6$, $V_1 = 0.3$, $V_2 = 0.5$, $V_3 = 30$, $\epsilon_1 = 2$, $\epsilon_2 = 0.9$, $\epsilon_3 = 5$, $R_1 = 10$, $R_2 = 20$, $T_{12} = 19$, $T_{23} = 25$, $\mu_1 = 1000$, $\mu_3 = 500$, $\nu_1 = 1000$ and $\nu_2 = 100$.

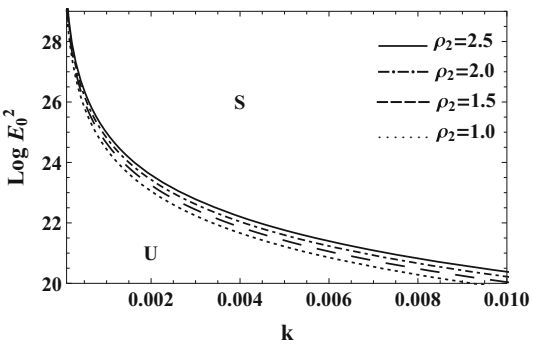

Figure 15. $a = 3$, $\rho_1 = 0.3$, $\rho_3 = 1.9$, $\xi_1 = 0.03$, $\xi_2 = 0.02$, $\xi_3 = 0.6$, $V_1 = 0.3$, $V_2 = 0.5$, $V_3 = 30$, $\epsilon_1 = 2$, $\epsilon_2 = 0.9$, $\epsilon_3 = 5$, $R_1 = 10$, $R_2 = 20$, $T_{12} = 19$, $T_{23} = 25$, $\mu_1 = 1000$, $\mu_3 = 500$, $\nu_1 = 1000$, $\nu_2 = 100$ and $\nu_3 = 600$.

the increase of V_2 has a stabilising influence. This role is enhanced for large values of k. The influence of the Darcy's coefficient ν_1 is depicted in figure 9. It is shown that this parameter has a stabilising influence, especially at small values of k. In contrast with the previous figure, the parameter ν_2, as depicted in figure 10, has a destabilising role. This role is enhanced at large values

of k. In figure 11, the influence of dynamic viscosity μ_3 is depicted and the dynamic viscosity has a destabilising effect, especially at large values k. Figure 12 shows the influence of the radius of the inner cylinder a has a dual role in the stability figure.

Finally, in asymmetric mode ($m = 1$), we show the influence of porosity of ξ_1 in figure 13. It is shown that this parameter has a stabilising influence. The influence of the Darcy's coefficient ν_3 is shown in figure 14. It is shown that this parameter has a destabilising influence. Figure 15 shows that the density of the middle fluid ρ_2 has a destabilising influence.

7. Concluding remarks

The aim of this work is to make a mathematical simplification to the problem of EHD stability of a vertical infinite cylindrical dielectric liquid sheet embedded between two different cylindrical liquids. All the fluids are saturated through porous media, where the porosity parameters of the media are taken into account. Because of various applications of the viscosity forces, the present study considers these parameters. The VPF theory is adopted to relax the mathematical manipulation of the analysis. Therefore, the viscous effect is demonstrated only through the normal stress conditions. Meanwhile, the fluids are considered as inviscid elsewhere. The normal mode technique is utilised to achieve the linear stability analysis. The present boundary-value problem leads to two coupled second-order ordinary differential equations with damped and complex coefficients. To simplify this analysis, the symmetric and antisymmetric modes are taken into account. Therefore, the coupled differential equations are combined into a single equation. The Routh–Hurwitz criteria are considered to govern the theoretical stability conditions. Upon appropriate data choices, the present study has recovered several special cases. This study examines the influence of uniform tangential electric field. The effect of tangential periodic electric fields will be considered in a subsequent paper. The numerical calculations are performed in the case of axisymmetric modes ($m = 0$) and also, the asymmetric mode ($m \neq 0$). In fact, in the former case, the following conclusions are reported:

1. the porosity has a stabilising effect,
2. Darcy's coefficients play a dual role on the stability figure. This role differs from ν_1 and ν_2,
3. the dynamic viscosity has a destabilising effect,
4. the streaming has a stabilising effect,
5. the thickness of the inner cylinder has a dual role. This role depends on the values of the wave number k.

In contrast, in the case of asymmetric modes ($m = 1$), we get the following conclusions:

1. the porosity has a stabilising effect,
2. Darcy's coefficients have a destabilising effect,
3. the density of the fluid has a destabilising effect.

Appendix A

For simplicity, we used this substituting for writing the coefficients,

$$
\begin{aligned}
M(A_1) &= I_{(m-1)}(kA_1) + I_{(m+1)}(kA_1),\\
L(A_1) &= K_{(m-1)}(kA_1) + K_{(m+1)}(kA_1),\\
P(A_1, A_2) &= I_{(m)}(kA_1)K_{(m)}(kA_2)\\
&\quad - I_{(m)}(kA_2)K_{(m)}(kA_1),\\
N(A_1, A_2) &= I_{(m)}(kA_1)L(A_2) - K_{(m)}(kA_1)M(A_2),\\
Q(A_1, A_2) &= I_{(m)}(kA_1)L(A_2) + K_{(m)}(kA_1)M(A_2),\\
S_I &= I_{(m-2)}(kA_1) + 2I_{(m)}(kA_1)\\
&\quad + I_{(m+2)}(kA_1),\\
S_K &= K_{(m-2)}(kA_1) + 2K_{(m)}(kA_1)\\
&\quad + K_{(m+2)}(kA_1),\\
U(A_1, A_2) &= L(A_1)M(A_2) - L(A_2)L(A_1),
\end{aligned}
$$

where A_1 and A_2 are a, b, R_1, R_2 and r. The values appearing in eqs (3.11)–(3.13) are listed as follows:

$$
\begin{aligned}
W &= \epsilon_2 N(R_1, R_1)P(a, R_1)(\epsilon_2 L(R_2)P(R_2, b)\\
&\quad + \epsilon_3 K_m(kR_2)N(b, R_2))\\
&\quad + \epsilon_1 K_{(m)}(ka)K_{(m)}(kR_1)M(R_1)\\
&\quad \times(\epsilon_2 N(R_1, R_2)P(R_2, b)\\
&\quad - \epsilon_3 N(b, R_2)P(R_2, R_1))\\
&\quad + L(R_1)(\epsilon_1 K_{(m)}(ka)K_{(m)}(kR_1)\\
&\quad + \epsilon_2 P(R_1, a))(\epsilon_2 N(R_1, R_2)P(R_2, b)\\
&\quad - \epsilon_3 N(b, R_2)P(R_2, R_1)),\\
L_1 &= \frac{2(\epsilon_1 - \epsilon_2)I_m(kR_1)}{W}\\
&\quad \times(\epsilon_2 N(R_1, R_2)P(R_2, b)\\
&\quad - \epsilon_3 N(b, R_2)P(R_2, R_1)),\\
L_2 &= \frac{2(\epsilon_2 - \epsilon_3)\epsilon_1 K_m(kR_1)N(R_1, R_1)P(R_2, b)}{W},\\
L_3 &= \frac{2(\epsilon_1 - \epsilon_2)}{N(R_1, R_1)\epsilon_2}\\
&\quad \times\left(-1 + \frac{\left[\begin{array}{l}\epsilon_1 K_m(kR_1)Q(a, R_1)(\epsilon_2 N(R_1, R_2)\\ \quad \times P(R_2, b) - \epsilon_3 N(b, R_2)\\ \quad P(R_2, R_1))\end{array}\right]}{W}\right),
\end{aligned}
$$

$$L_4 = \frac{\left[\begin{array}{c}(\epsilon_1-\epsilon_2)K_m(kR_1)P(R_1,a)(\epsilon_3 N(R_1,R_2)\\ \times P(R_2,b)-\epsilon_2 N(b,R_2)P(R_2,R_1))\end{array}\right]}{WN(R_1,R_1)},$$

$$L_5 = \frac{2\epsilon_1(\epsilon_3-\epsilon_2)K_m(kR_1)Q(a,R_1)P(R_2,b)}{W},$$

$$L_6 = \frac{2\epsilon_2(\epsilon_2-\epsilon_3)K_m(kR_1)P(a,R_1)P(R_2,b)}{W},$$

$$L_7 = \frac{2(\epsilon_2-\epsilon_1)}{\epsilon_2 N(R_1,R_1)P(R_2,b)} \times\Bigg(P(R_2,R_1)+\frac{K_m(kR_1)}{W}(\epsilon_1 P(R_2,R_1)Q(a,R_1) -\epsilon_2 P(a,R_1)Q(R_2,R_1))\times(\epsilon_2 N(R_1,R_2)P(R_2,b) -\epsilon_3 N(b,R_2)P(R_2,R_1))\Bigg),$$

$$L_8 = \frac{\left[\begin{array}{c}2(\epsilon_3-\epsilon_2)K_m(kR_1)(\epsilon_1 P(R_2,R_1)Q(a,R_1)\\ +\epsilon_2 P(R_1,a)Q(R_2,R_1))\end{array}\right]}{\epsilon_2 N(R_1,R_1)P(R_2,b)}.$$

Appendix B

The coefficients appearing in eqs (3.24) and (3.25) are listed as follows:

$$k_{11} = \frac{2Q(R_1,a)\rho_1}{k\xi_1 U(R_1,a)} - \frac{2Q(R_1,R_2)\rho_2}{k\xi_2 U(R_2,R_1)},$$

$$q_{22} = -\frac{2Q(R_1,R_1)\rho_2}{k\xi_2 U(R_2,R_1)},$$

$$f_{11} = \frac{\left[\begin{array}{c}2(Q(R_1,a)\nu_1+\mu_1(S_I(R_1)L(a)\\ +S_K(R_1)M(a)))\end{array}\right]}{kU(R_1,a)} + \frac{\left[\begin{array}{c}2(Q(R_1,R_2)\nu_2+\mu_2(S_I(R_1)L(R_2)\\ +S_K(R_1)M(R_2)))\end{array}\right]}{kU(R_1,R_2)},$$

$$l_{11} = \frac{2V_1\rho_1(1+\xi_1)Q(R_1,a)}{\xi_1^2 U(R_1,a)} - \frac{2V_2\rho_2(1+\xi_2)Q(R_1,R_2)}{\xi_2^2 U(R_2,R_1)},$$

$$s_{11} = kE_0^2((P(R_1,R_1)(L_3+L_5) +Q(R_1,R_1)(L_4+L_6))\epsilon_2-\epsilon_1 P(a,R_1)L_1) - \frac{2kQ(R_1,a)\rho_1 V_1^2}{\xi_1^2 U(R_1,a)} + \frac{2kQ(R_1,R_2)\rho_2 V_2^2}{\xi_2^2 U(R_2,R_1)} - \frac{(k^2R_1^2-1)T_{12}}{R_1^2},$$

$$h_{11} = \frac{\left[\begin{array}{c}2Q(R_1,a)V_1\nu_1+V_1\mu_1 k^2(M(a)S_K(R_1)\\ +L(a)S_I(R_1))\end{array}\right]}{U(R_1,a)} - \frac{\left[\begin{array}{c}2Q(R_1,R_2)V_2\nu_2+V_2\mu_2 k^2(M(R_2)S_K(R_1)\\ +L(R_2)S_I(R_1))\end{array}\right]}{U(R_2,R_1)},$$

$$f_{22} = \frac{\left[\begin{array}{c}2Q(R_1,R_1)\nu_2+2\mu_2(S_I(R_1)L(R_1)\\ +S_K(R_1)M(R_1))\end{array}\right]}{kU(R_1,R_2)},$$

$$l_{22} = \frac{2V_2\rho_2(1+\xi_2)Q(R_1,R_1)}{\xi_2^2 U(R_1,R_2)},$$

$$s_{22} = -k\,\epsilon_1 E_0^2 P(a,R_1)L_2 + \frac{2kQ(R_1,R_1)\rho_2 V_2^2}{\xi_2^2 U(R_2,R_1)},$$

$$h_{22} = \frac{\left[\begin{array}{c}2Q(R_1,R_1)V_2\nu_2+2V_2\mu_2 k^2(M(R_1)S_K(R_1)\\ +L(R_1)S_I(R_1))\end{array}\right]}{U(R_1,R_2)},$$

$$q_{21} = \frac{2Q(R_2,R_2)\rho_2}{k\xi_2 U(R_2,R_1)},$$

$$k_{12} = \frac{2Q(R_2,R_1)\rho_2}{k\xi_2 U(R_2,R_1)} - \frac{2Q(R_2,b)\rho_3}{k\xi_3 U(R_2,b)},$$

$$f_{12} = \frac{\left[\begin{array}{c}2(Q(R_2,R_1)\nu_2+\mu_2(S_I(R_2)L(R_1)\\ +S_K(R_2)M(R_1)))\end{array}\right]}{kU(R_2,R_1)} + \frac{2(Q(R_2,b)\nu_3+\mu_3(S_I(R_2)L(b)+S_K(R_2)M(b)))}{kU(b,R_2)},$$

$$l_{12} = \frac{2V_2\rho_2(1+\xi_2)Q(R_2,R_1)}{\xi_2^2 U(R_2,R_1))} + \frac{2V_3\rho_3(1+\xi_3)Q(R_2,b)}{\xi_3^2 U(b,R_2)},$$

$$s_{12} = k\,\epsilon_3 E_0^2 P(b,R_2)L_8 + \frac{2kQ(R_2,R_1)\rho_2 V_2^2}{\xi_2^2 U(R_1,R_2)} - \frac{(k^2R_2^2-1)T_{23}}{R_2^2} + \frac{2kQ(R_2,b)\rho_3 V_3^2}{\xi_3^2 U(R_2,b)},$$

$$h_{12} = \frac{\left[\begin{array}{c}2Q(R_2,R_1)V_2\nu_2+V_2\mu_2 k^2(M(R_1)S_K(R_2)\\ +L(R_1)S_I(R_2))\end{array}\right]}{U(R_2,R_1)} + \frac{\left[\begin{array}{c}2Q(R_2,b)V_3\nu_3+V_3\mu_3 k^2(M(b)S_K(R_2)\\ +L(b)S_I(R_2))\end{array}\right]}{U(b,R_2)},$$

$$f_{21} = \frac{\left[\begin{array}{c}2Q(R_1,R_1)\nu_2+2\mu_2(S_I(R_2)L(R_2)\\ +S_K(R_2)M(R_2))\end{array}\right]}{kU(R_2,R_1)},$$

$$l_{21} = \frac{2V_2\rho_2(1+\xi_2)Q(R_2,R_2)}{\xi_2^2 U(R_2,R_1)},$$

$$s_{21} = kE_0^2((P(R_2, R_1)(L_3 + L_5) + Q(R_2, R_1)(L_4 + L_6))\epsilon_2 - \epsilon_3 P(b, R_2)L_7) - \frac{2kQ(R_2, R_2)\rho_2 V_2^2}{\xi_2^2 U(R_2, R_1)},$$

$$h_{21} = \frac{\left[\begin{array}{l} 2Q(R_2, R_2)V_2\nu_2 + 2V_2\mu_2 k^2(M(R_2)S_K(R_2) \\ \quad + L(R_2)S_I(R_2)) \end{array}\right]}{U(R_2, R_1)}.$$

Appendix C

The coefficients appearing in eqs (5.2) and (6.4) are listed as follows:

$$\tilde{k}_{11} = \frac{2Q(R_1, a)\rho_1}{kU(R_1, a)} - \frac{2Q(R_1, R_2)\rho_2}{kU(R_2, R_1)},$$

$$\tilde{q}_{22} = -\frac{2Q(R_1, R_1)\rho_2}{kU(R_2, R_1)}, \quad \tilde{q}_{21} = \frac{2Q(R_2, R_2)\rho_2}{kU(R_2, R_1)},$$

$$\tilde{k}_{12} = \frac{2Q(R_2, R_1)\rho_2}{kU(R_2, R_1)} - \frac{2Q(R_2, b)\rho_3}{kU(R_2, b)},$$

$$\alpha_1 = \frac{\left[\begin{array}{l} (Jk((P(R_1, R_1)(L_3 + L_5) \\ \quad + Q(R_1, R_1)(L_4 + L_6))\epsilon_2 - \epsilon_1 P(a, R_1)L_1) \\ \quad - k\epsilon_1 P(a, R_1)L_2) \end{array}\right]}{2(\tilde{q}_{22} + J\tilde{k}_{11})} + \frac{\left[\begin{array}{l} (k\epsilon_3 P(b, R_2)L_8) + Jk((P(R_2, R_1)(L_3 + L_5) \\ \quad + Q(R_2, R_1)(L_4 + L_6))\epsilon_2 - \epsilon_3 P(b, R_2)L_7) \end{array}\right]}{2(\tilde{k}_{12} + J\tilde{q}_{21})},$$

$$\beta_1 = -\frac{Jk^2(R_1^2 - 1)T_{12}}{2R_1^2(\tilde{q}_{22} + J\tilde{k}_{11})} - \frac{(k^2R_2^2 - 1)T_{23}}{2R_2^2(\tilde{k}_{12} + J\tilde{q}_{21})},$$

$$\beta = H_3^2 - G_3F_3H_3 + \frac{G_3^2}{2(q_{22} + Jk_{11})}\left(\frac{2kQ(R_1, R_1)\rho_2 V_2^2}{\xi_2^2 U(R_2, R_1)} - J\left(\frac{2kQ(R_1, a)\rho_1 V_1^2}{\xi_1^2 U(R_1, a)} - \frac{2kQ(R_1, R_2)\rho_2 V_2^2}{\xi_2^2 U(R_2, R_1)} + \frac{(k^2R_1^2 - 1)T_{12}}{R_1^2}\right)\right) + \frac{G_3^2}{2(k_{212} + Jq_{21})}\left(\frac{2kQ(R_2, R_1)\rho_2 V_2^2}{\xi_2^2 U(R_1, R_2)} - \frac{(k^2R_2^2 - 1)T_{23}}{R_2^2} + \frac{2kQ(R_2, b)\rho_3 V_3^2}{\xi_3^2 U(R_2, b)} - J\left(\frac{2kQ(R_2, R_2)\rho_2 V_2^2}{\xi_2^2 U(R_2, R_1)}\right)\right).$$

References

[1] J Eggers and E Villermaux, *Rep. Prog. Phys.* **71**, 036601 (2008)

[2] G Amini, Y Lv, A Dolatabadi and M Ihme, *Phys. Fluids* **26**, 114105 (2014)

[3] S Chandrasekhar, *Hydrodynamic and hydromagnetic stability* (Clarendon Press, Oxford, 1961)

[4] A R Seadawy and K El-Rashidy, *Pramana – J. Phys.* **87**: 20 (2016)

[5] C H Chen, *Electrokinetics and electrohydrodynamics in microsystems* edited by Ramos (Springer, New York, 2011)

[6] S Korkut, D A Saville and I A Akasy, *Phys. Rev. Lett.* **100**, 034503 (2008)

[7] M F Elsayed, G M Moatimid, F M F Elsabaa and M F E Amer, *J. Porous Media* **19**, 751 (2016)

[8] G M Moatimid, *Phys. Scr.* **79**, 065403 (2009)

[9] K Vafai, *Handbook of porous media* 2nd edn (CRC Press, Taylor and Francis Group, Boca Raton, 2005)

[10] M F El-Sayed, G M Moatimid, F M F Elsabaa and M F E Amer, *Atomization Sprays* **26**, 349 (2016)

[11] A E K Elcoot and G M Moatimid, *Physica A* **343**, 15 (2004)

[12] G M Moatimid, *Physica A* **328**, 525 (2003)

[13] D D Joseph, *Int. J. Multiphase Flow* **32**, 285 (2006)

[14] G M Moatimid and M A Hassan, *Math. Probl. Eng.* **2013**, 416562 (2013)

[15] G M Moatimid, M A Hassan and B E M Tantawy, *J. Nat. Sci. Math.* **7**, 129 (2014)

[16] G M Moatimid and M A Hassan, *Int. J. Eng. Sci.* **54**, 15 (2012)

[17] M K Awasthi, *Eur. Phys. J. Plus* **129**, 78 (2014)

[18] F Li, O Ozen, N Aubry and D T Papageorgiou, *J. Fluid Mech.* **583**, 347 (2007)

[19] J R Melcher, *Field coupled surface waves* (MIT Press, Cambridge, MA, 1963)

[20] N T El-Dabe, E F El-Shehawey, G M Moatimid and A A Mohamed, *J. Math. Phys.* **26**, 2072 (1985)

[21] Z Zahreddin and E F El-Shehawey, *Indian J. Pure Appl. Math.* **19**, 963 (1988)